



Crustal thickness, Poisson's ratio and Moho sharpness beneath Tien Shan: Constraints from receiver functions analysis



Outline:

- ❑ **Objectives.**
- ❑ **Motivations.**
- ❑ **Geological setting.**
- ❑ **Previous investigations.**
- ❑ **Data & methods.**
- ❑ **Observations.**
- ❑ **Interpretation.**
- ❑ **Conclusions.**

Objectives:

To identify new constraints on the composition and structure of Tien Shan by measuring:

- 1. Crustal thickness (H).**
- 2. Poisson's ratio (σ) , which can be determine from the ratio of (V_p/V_s) or (Φ), $\sigma=0.5[1-1/(\Phi*\Phi-1)]$.**
- 3. Moho sharpness (R).**

Motivations:

- ◆ **Tien Shan is considered to be one of the most tectonically active mountain ranges in the world.**
- ◆ **Tien Shan is one of the most active seismic regions worldwide, four events occurred with magnitude exceeding (8) in this century.**
- ◆ **Tien Shan has a high rate of deformation which leads scholars to investigate the causes of it.**
- ◆ **Most of previous studies investigate the mantle structure, still not many focus of the composition and structure of the crust.**

Geological Setting:

▲ Tien Shan is a chain of mountains range located in Central Asia and extends approximately east-west for almost (2500) km long and wide of (300-500) km and has a maximum elevation of (7000) m.

▲ The Tien Shan is at the boundary between the active structures of the northern Tarim Basin and the stable Kazakh Shield.

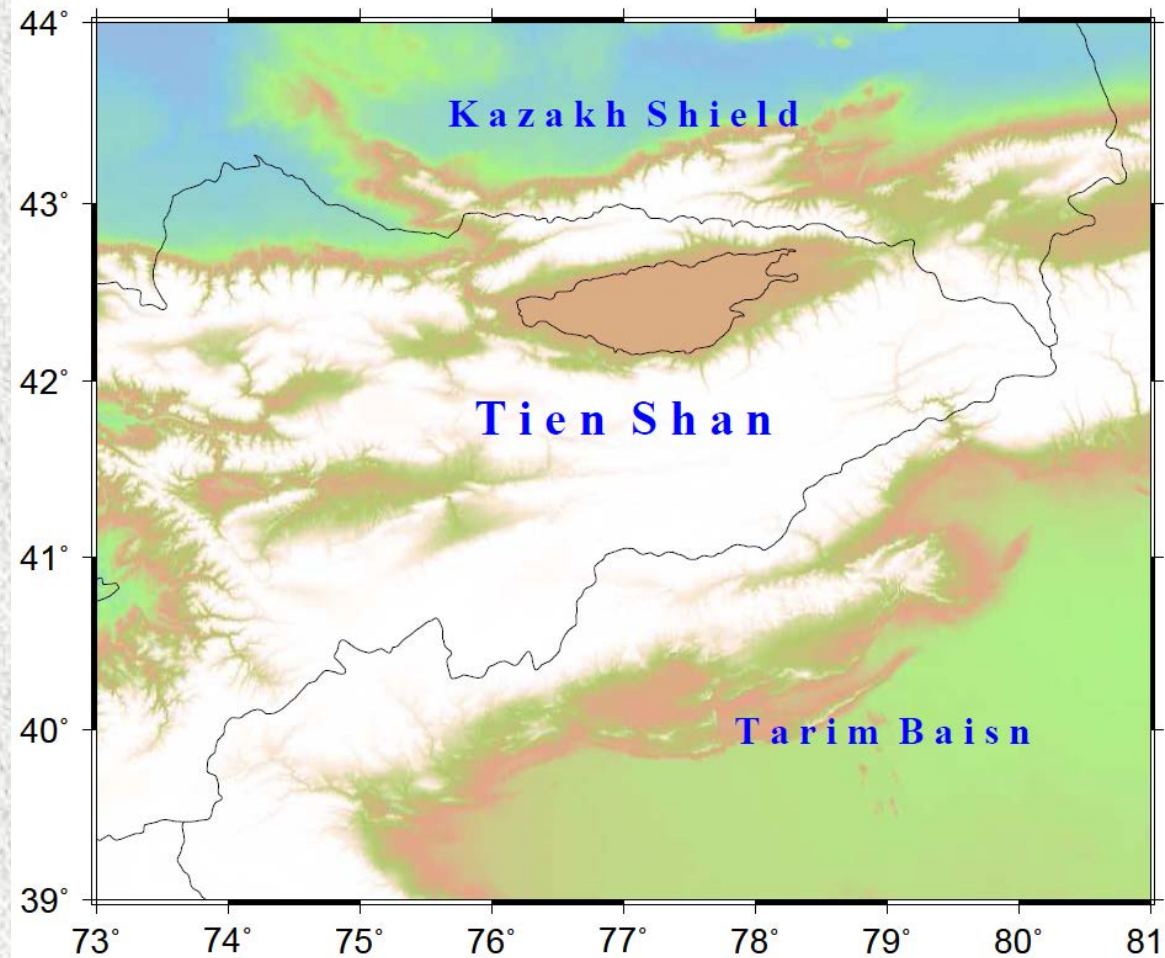


Figure 1: Topographic map of Tien Shan

△ Tien Shan was formed by convergence of a few continental blocks during the late Palaeozoic.

△ Tectonic activity resumed at about (20) Ma, and at the present, the central Tien Shan is shortening at a rate of about (20) mm/year.

△ Igneous rocks can be observed over the north and east of the Tien Shan.

△ While the southern and western parts of the Tien Shan consist of meta-sedimentary rocks.

△ The basins which lie between the mountains of Tien Shan are filled with younger sediments.

△ Strike-slip and normal fault types appear to have characterized much of the Tien Shan area.

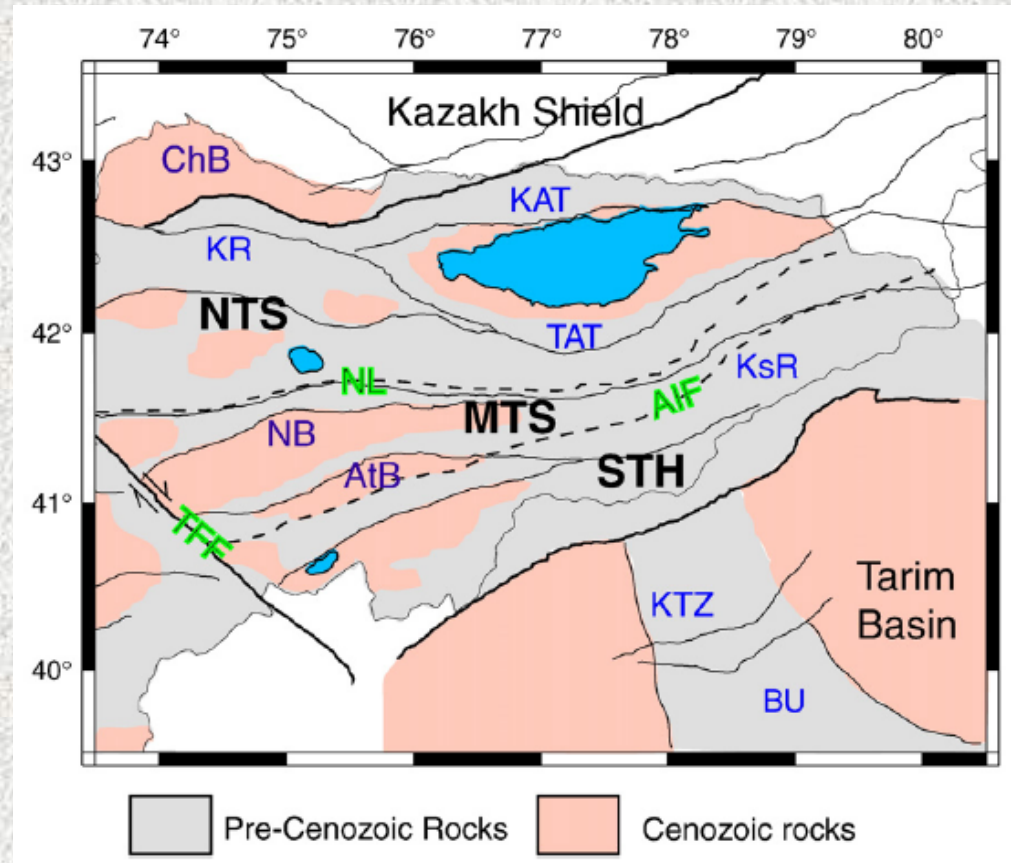


Figure 2: Geological map of Tien Shan
[Omuralieva, A. et al., 2009]

△ The Tien Shan record two Paleozoic collisional events:
1. Along the southern margin
2. Along the northern margin

△ Tectonics of the Tien Shan are dominated by:
1. Thrusting on (E-W) striking faults.
2. Folding of Cenozoic sediments compose of (E-W) trending mountain ranges.

△ Quite a few of scholars suggest that the Tarim Basin is being thrust under the Tien Shan.

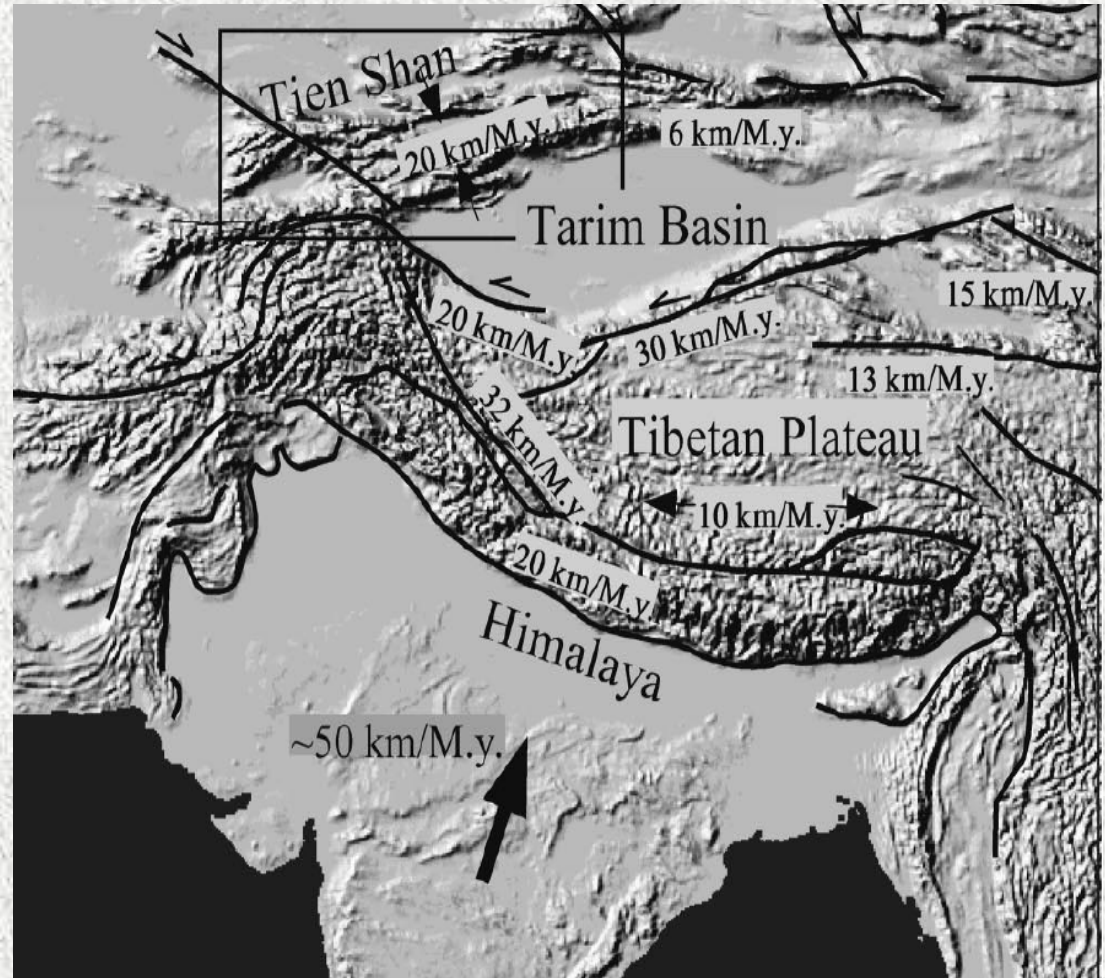


Figure 3: Regional tectonic map of Central Asia
[Bullen, M. et al., 2001]

Previous Investigations:

- The average crustal thickness is (50-55) km and it thickens to the south to the Tibetan Plateau.
- The western areas, as compared to the eastern ones separated by the Talas-Fergana Fault, are characterized by higher velocities in the upper mantle.
- The crust in the central Tien Shan is underlain by a high-velocity cover (mantle lithosphere) several tens kilometers thick.

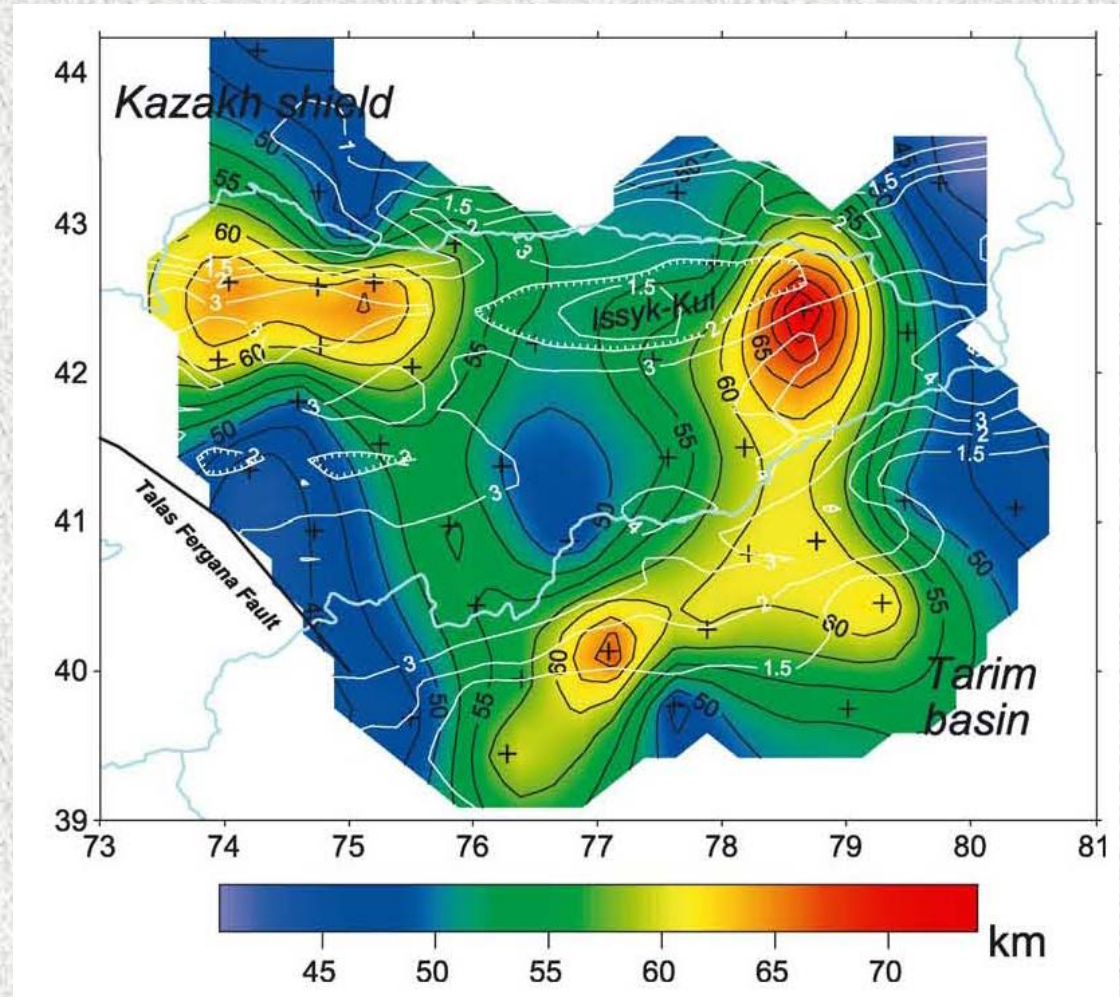


Figure 4: Crustal thickness of Tien Shan
[Vinnik, L. et al., 2004]

- ▣ The crustal thickness is largest (about 60 km) in the Tarim–Tien Shan junction zone.
- ▣ They identify low velocity anomalies in the upper layer of the mantle as a result from the delamination of the subcrustal lithosphere.
- ▣ They suggest the presence of a small plume in the upper mantle of the Tien Shan.

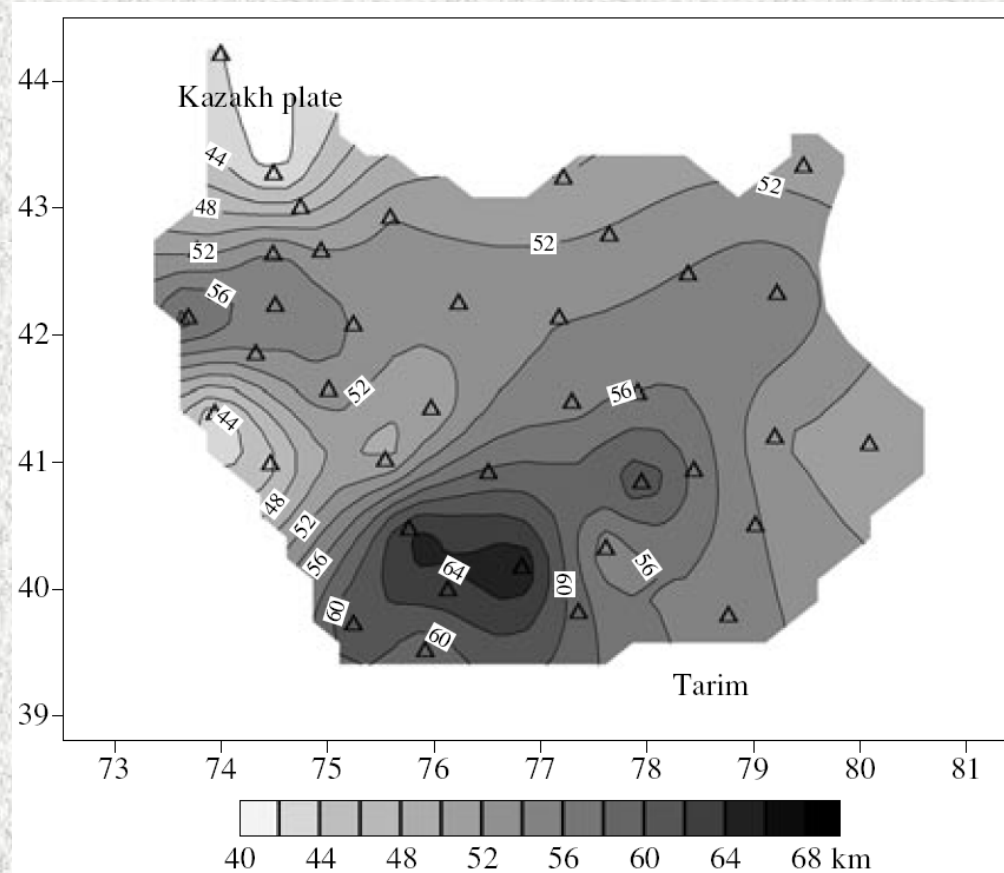


Figure 5: Crustal thickness of Tien Shan
[Vinnik, L. et al., 2006]

- ✧ The upper crust has a greatly varied thickness, as thick as (30-36) km on the two sides of the Tien Shan Mountains and as thin as (20-25) km beneath the center.
- ✧ The velocity of the lower crust is (6.6-6.9) km/s and the horizontal variation of the velocity is evident, (6.6) km/s on the two sides of the Tien Shan and (6.9) km/s beneath the central part of it.
- ✧ The Moho beneath the Tien Shan Mountains is possibly a young newly formed due to the collision.
- ✧ The low-velocity zone in the crust varies greatly in depth, which may indicate a superimpose detachment zone.

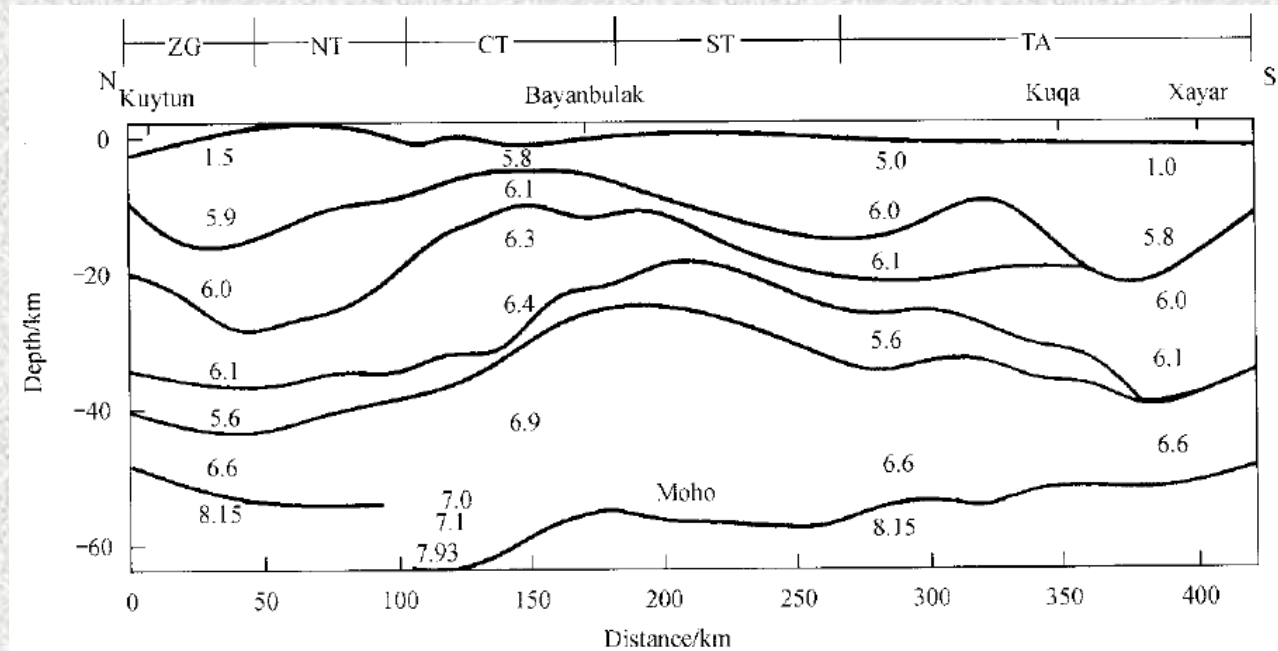


Figure 6: Velocity structure of Tien Shan
[Deyuan, L. et al., 2000]

- ✘ They confirm the presence of a thin (less than about 100 km depth) lithospheric beneath the central part.
- ✘ They observation a low P- wave velocity structure in the upper mantle of Tien Shan.
- ✘ They suggest that the Tien Shan may represent an area of active lithospheric delamination.

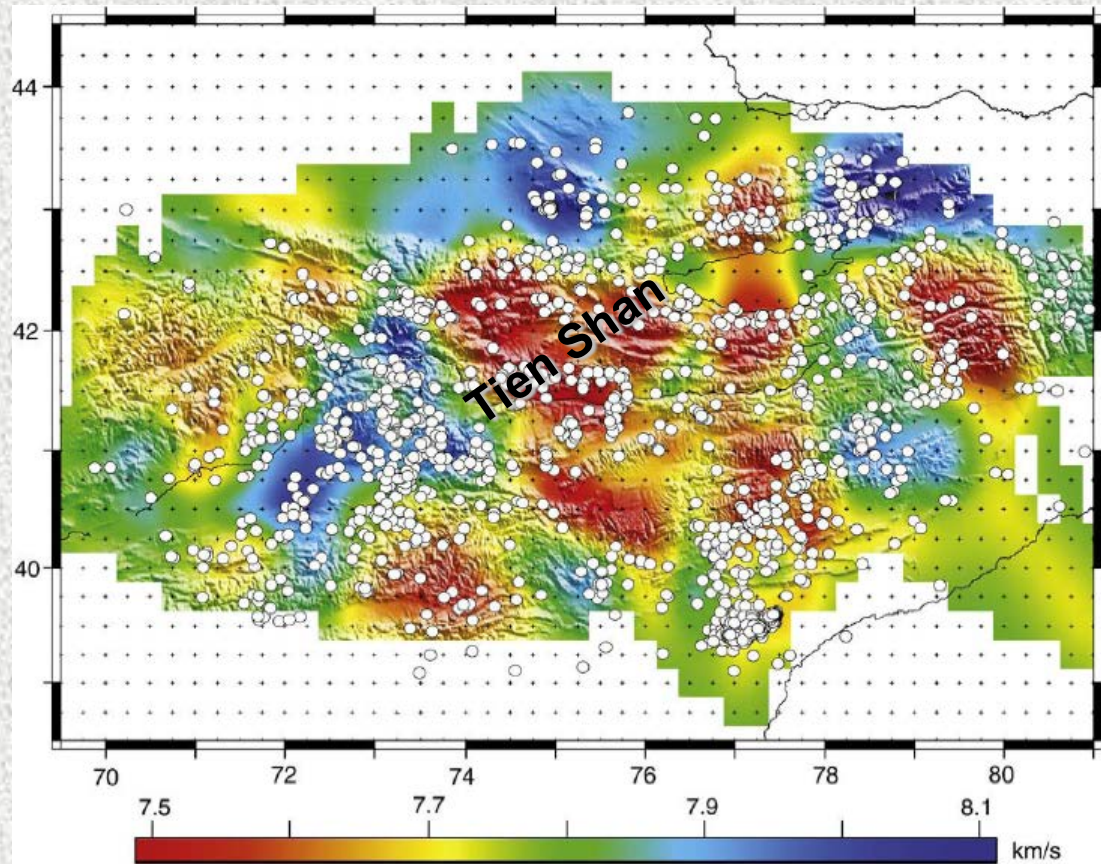


Figure 7: Velocity structure of Tien Shan
[Zhiwei, L. et al., 2009]

Data & methods:

- The data set used in this study consist of primarily of teleseismic data recorded by (20) broadband stations in Tien Shan.
- The data was obtained from IRIS (Incorporated Research Institutions for Seismology) DMC (Data Management Center).
- The events occurred during (1985) to (2010) with epicentral distance range from (30°) to (180°).

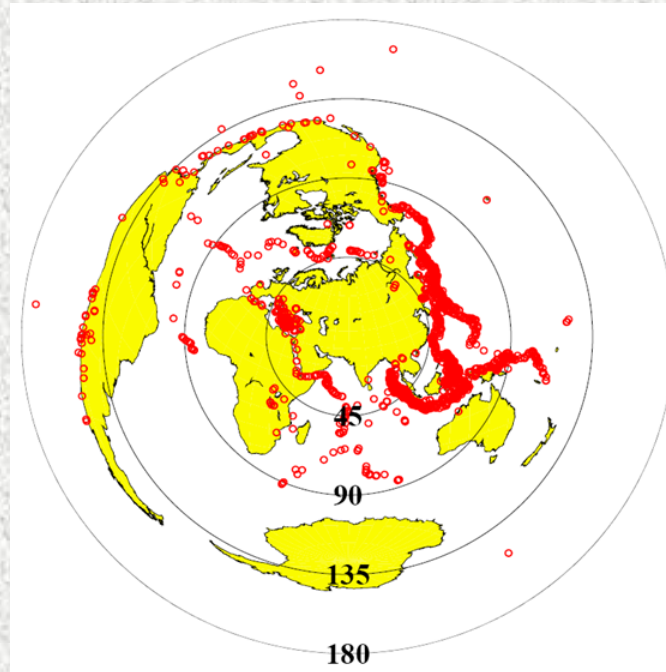


Figure 8: Locations of the events used in this study

Receiver functions analysis (RFs):

- ▲ Receiver function analysis is the method for studying the crust and the upper-mantle discontinuities.
- ▲ It can detect discontinuities beneath a seismic station by identifying P-to-S converted waves.
- ▲ It can be calculated by de-convolving the vertical from the radial and tangential components.

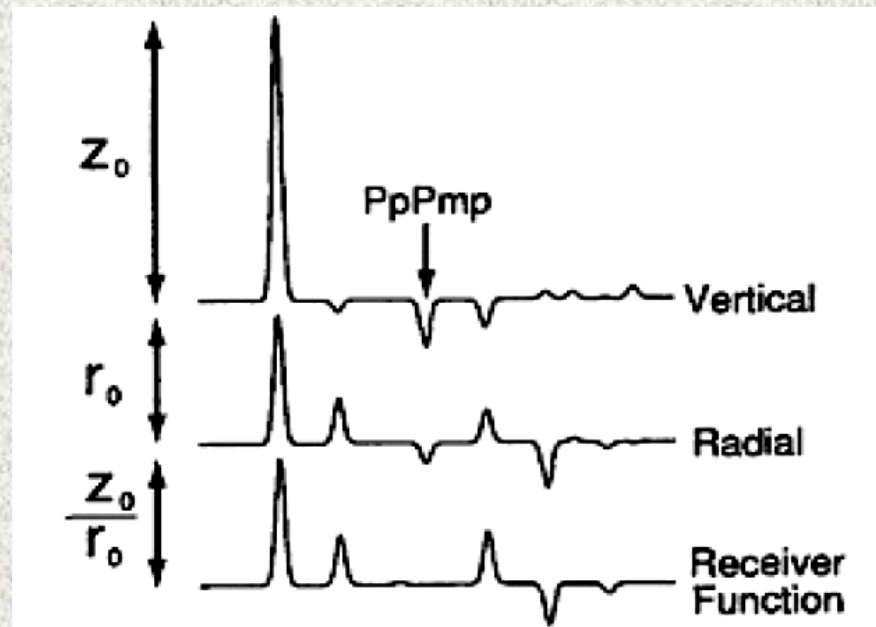


Figure 9: The vertical and radial components

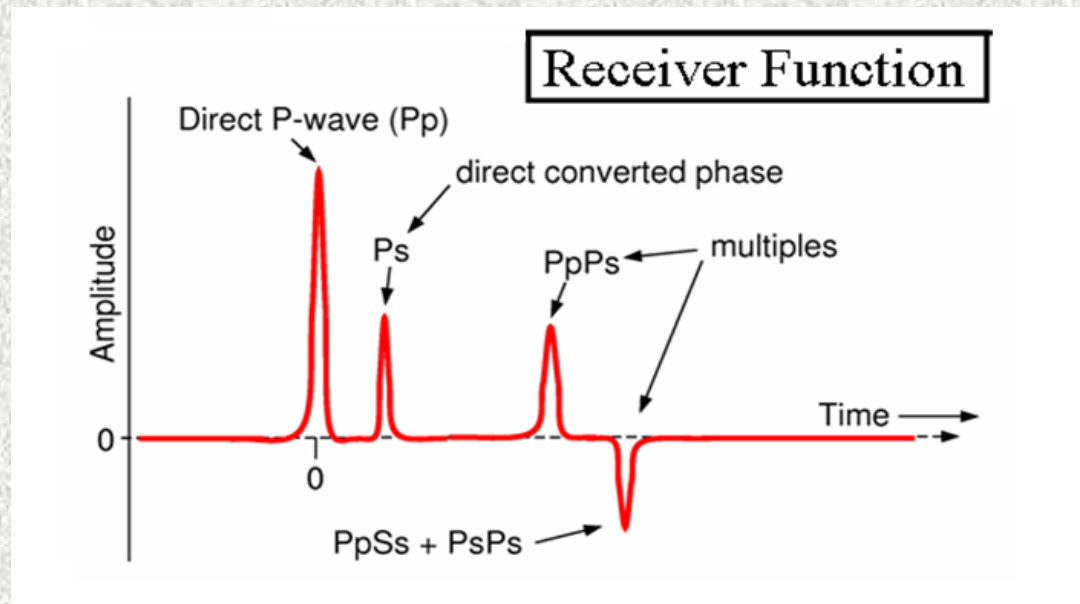


Figure 11: P-to-S converted phases

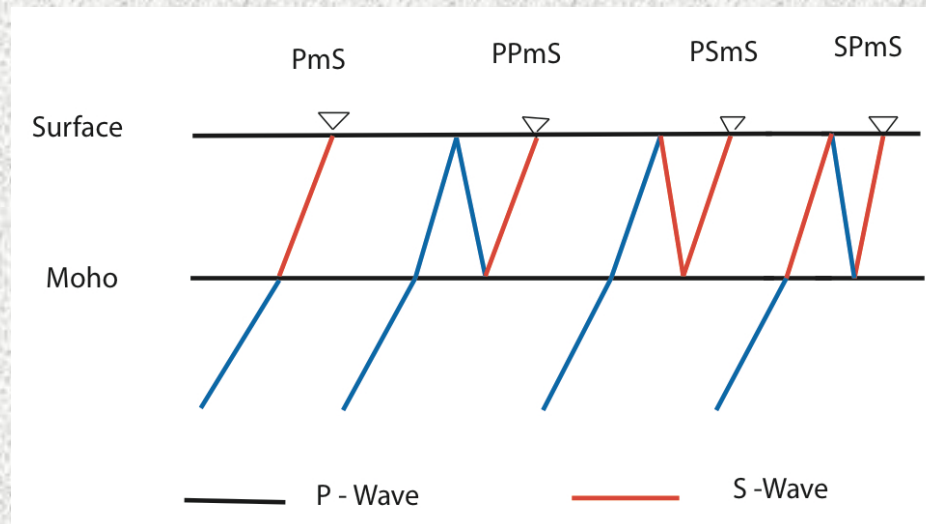


Figure 12: The raypaths for the converted phases.

After deconvolution :

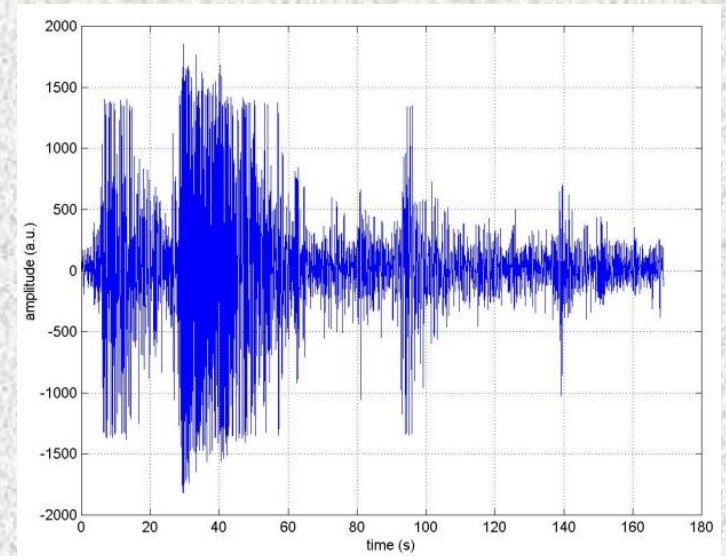


Figure 13: Original radial component seismograms

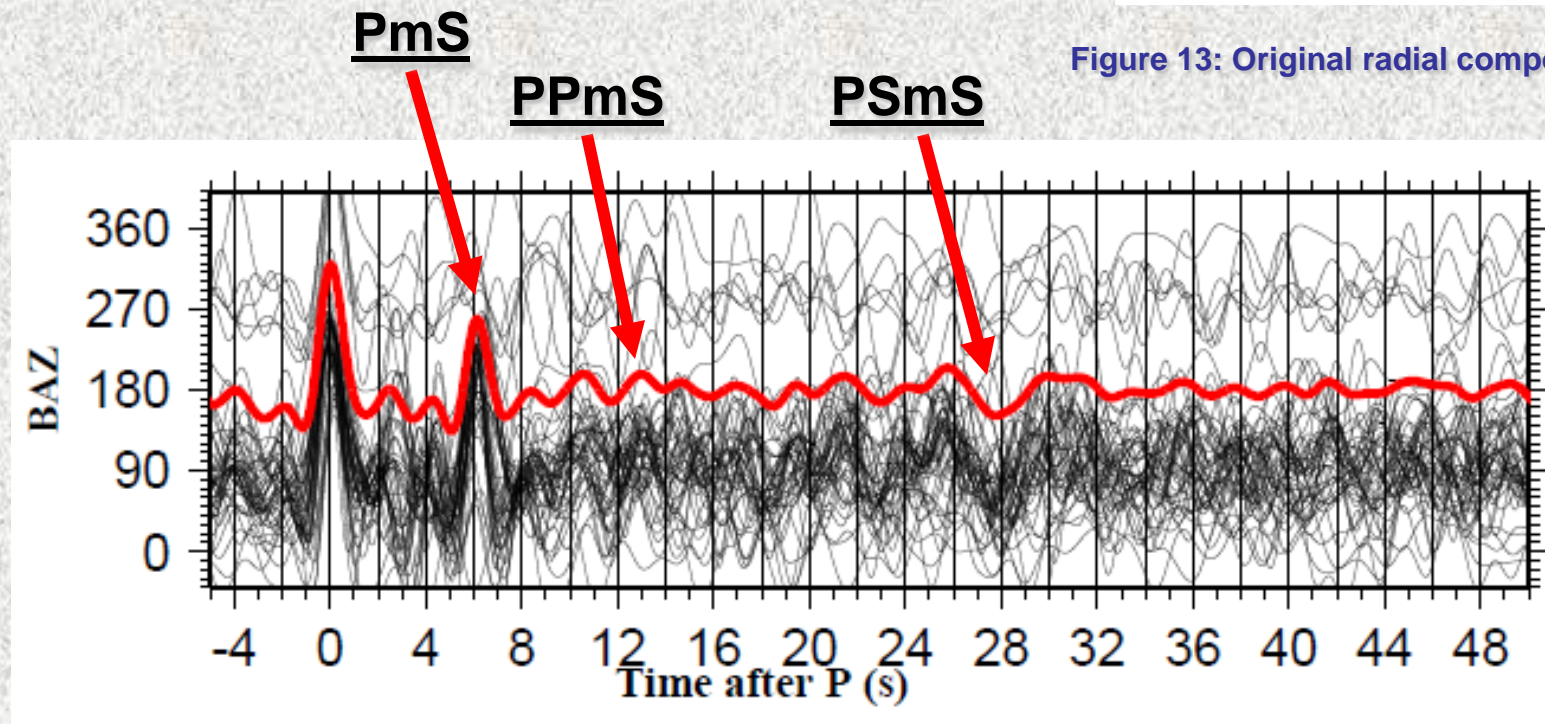


Figure 14: Observation of P-to-S converted waves

♦ The study applied the method of Zhu and Kanamori (2000) for the stacking of receiver functions by the following steps:

1) Selecting a P-wave velocity model for the study area ($V_p=6.1$ km/s) based on Martynov et al., [2004].

2) Dividing the top-60 or so km of the earth beneath a station into thin layers (e.g., 1 km thick).

3) By assuming that the Moho is located at the bottom of each of the thin layers, the receiver functions recorded by the station are move-out corrected from the following equations [Nair et al., 2006]:

$$t_1^{(i,j)} = \int_{-H_i}^0 [\sqrt{(V_p(z)/\phi_j)^{-2} - p^2} - \sqrt{V_p(z)^{-2} - p^2}] dz \quad (1)$$

$$t_2^{(i,j)} = \int_{-H_i}^0 [\sqrt{(V_p(z)/\phi_j)^{-2} - p^2} + \sqrt{V_p(z)^{-2} - p^2}] dz \quad (2)$$

$$t_3^{(i,j)} = \int_{-H_i}^0 2\sqrt{(V_p(z)/\phi_j)^{-2} - p^2} dz \quad (3)$$

□ Where t_1 , t_2 , and t_3 is for PmS, PPmS, and PSmS, respectively, H_i is the depth of the bottom of the i -th layer, and p is the real ray-parameter in sec/degree.

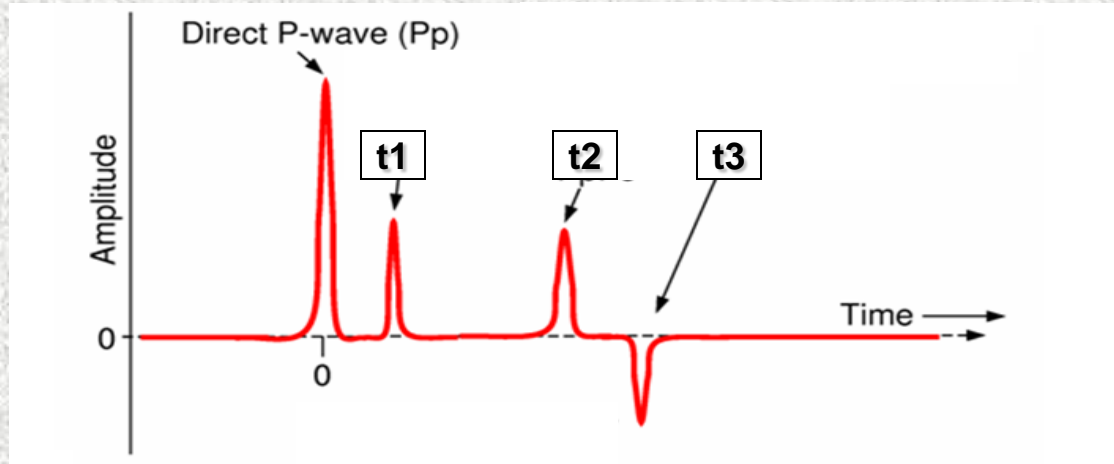


Figure 15: Original radial component seismograms

- ◆ **The receiver functions at each of the stations will be stacked using:**

$$A(H_i, \phi_j) = \sum_{k=1}^n w_1 S_k(t_1^{(i,j)}) + w_2 S_k(t_2^{(t,j)}) - w_3 S_k(t_3^{(i,j)}) \quad (4)$$

- **Where $w_1 + w_2 + w_3 = 1$ are the weighting factors, n is the number of RFs participating in the stacking. And $S_k(t)$ is the amplitude of the point after the first P arrival.**

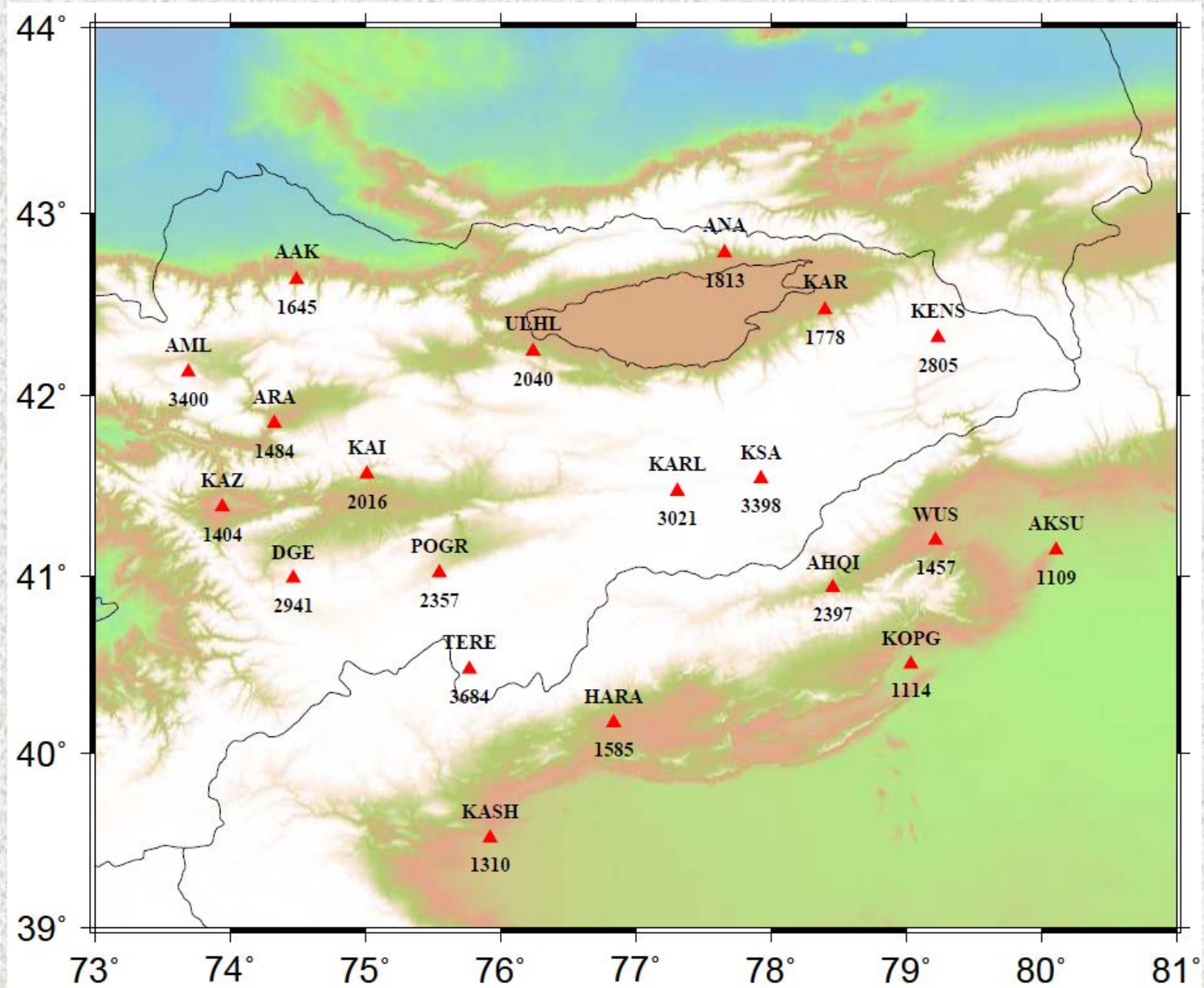


Figure 10: Locations of seismic stations with the elevation

Observations:

On the basis of the quality of the original receiver functions, the stations have been divided into two categories:

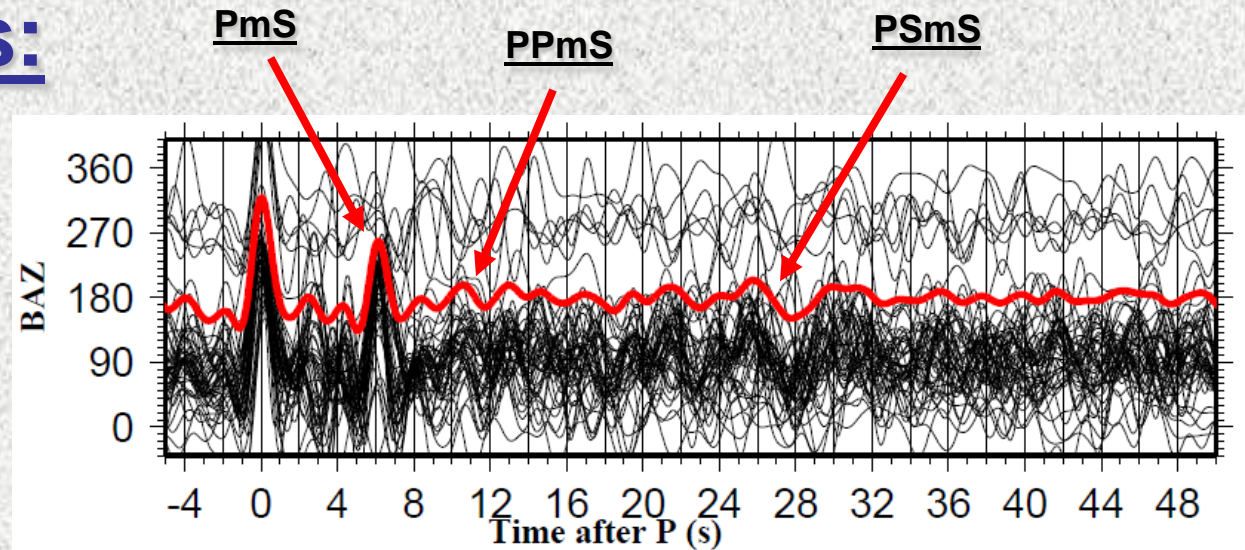


Figure 16: Category (A) show clear PmS, PPmS and PSmS arrivals

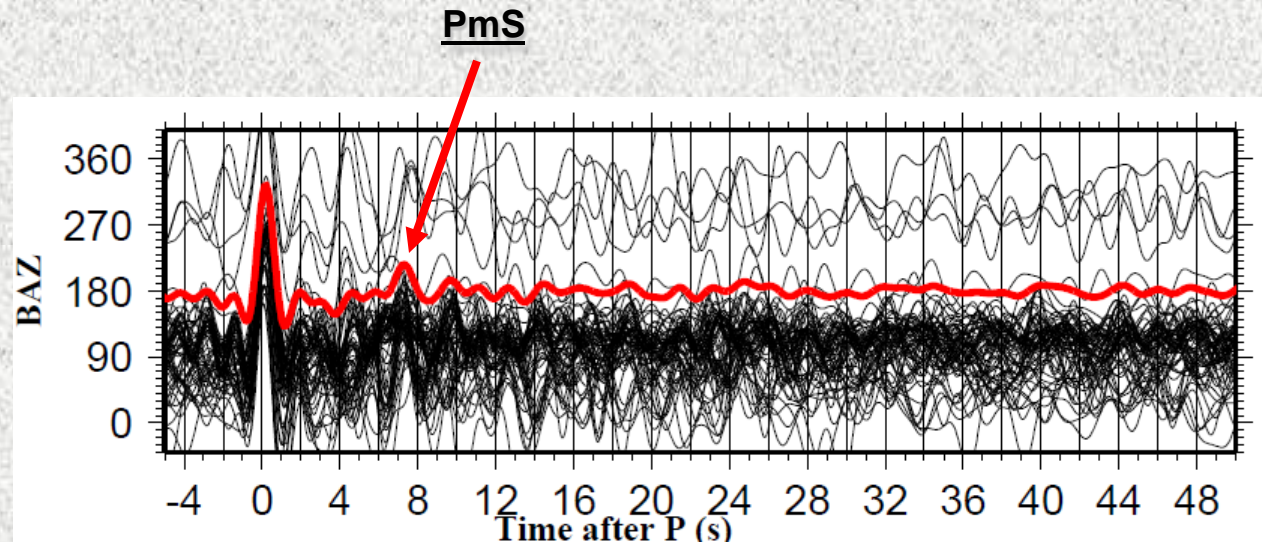
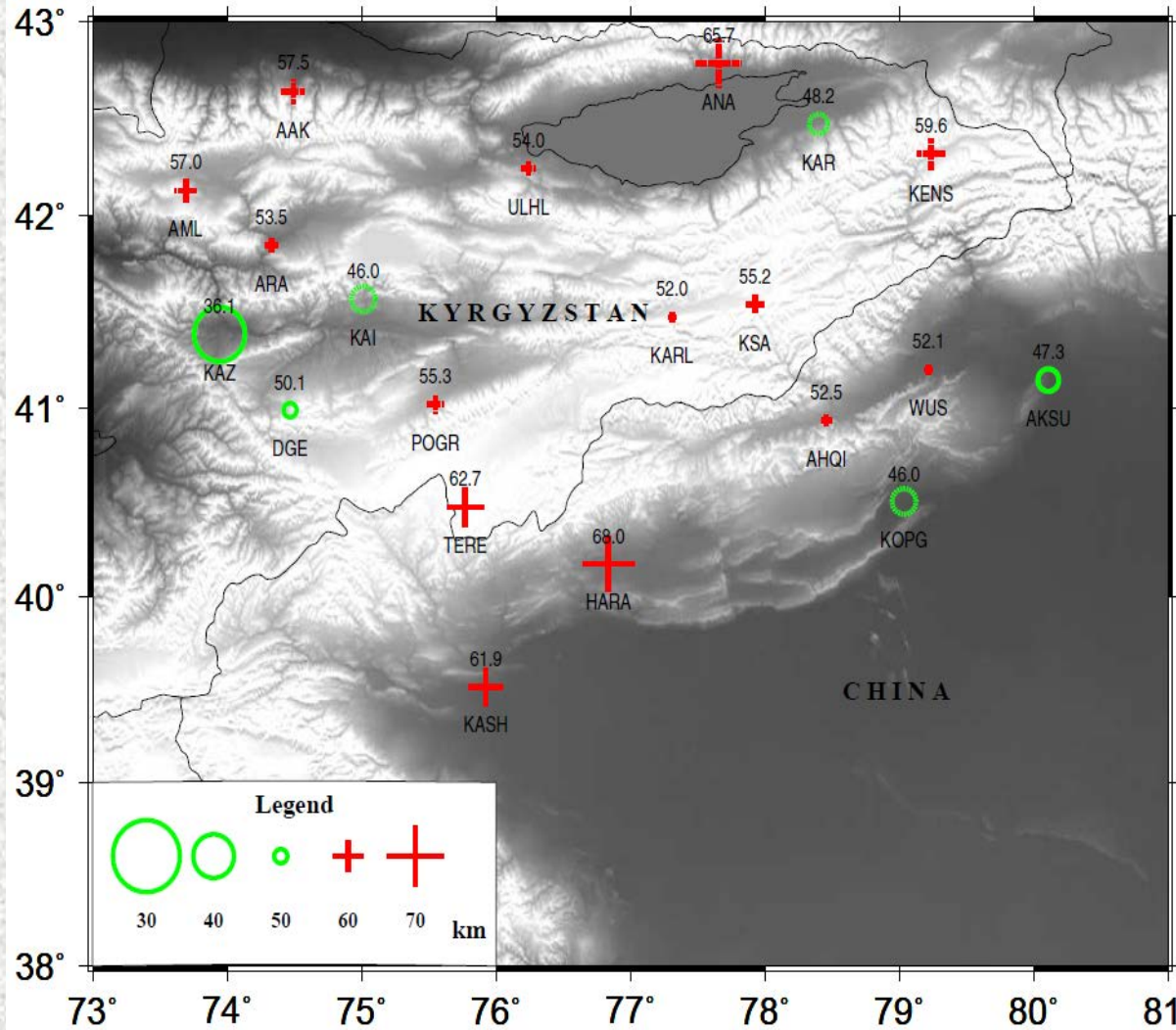


Figure 17: Category (B) show clear PmS but neither PPmS or PSmS, thus \emptyset cannot be determined clearly; H can be fairly estimated by assuming a normal \emptyset of (1.80).

#	Station	H	R	σ	VpVs	Category
1	ARA	53.5	0.13	0.276785714	1.8	A
2	KAZ	36.1	0.281	0.291695829	1.844	
3	DGE	50.1	0.307	0.246472931	1.724	
4	KARL	52	0.182	0.279625398	1.808	
5	TERE	62.7	0.134	0.2817162	1.814	
6	KASH	61.9	0.336	0.286135507	1.827	
7	HARA	68	0.194	0.293601651	1.85	
8	WUS	52.1	0.113	0.258804713	1.753	
9	KSA	55.2	0.229	0.285465272	1.825	
10	AKSU	47.3	0.098	0.278213072	1.804	
11	AML	57	0.102	-	1.8	B
12	AAK	57.5	0.129			
13	KAI	46	0.133			
14	ULHL	54	0.084			
15	ANA	65.7	0.204			
16	AHQI	52.5	0.105			
17	KENS	59.6	0.122			
18	KOPG	46	0.267			
19	KAR	48.2	0.24			
20	POGR	55.3	0.085			

Table 1: Observations of crustal thickness (H), (Vp/Vs) and Moho sharpness (R) for all stations

Crustal thickness (H):



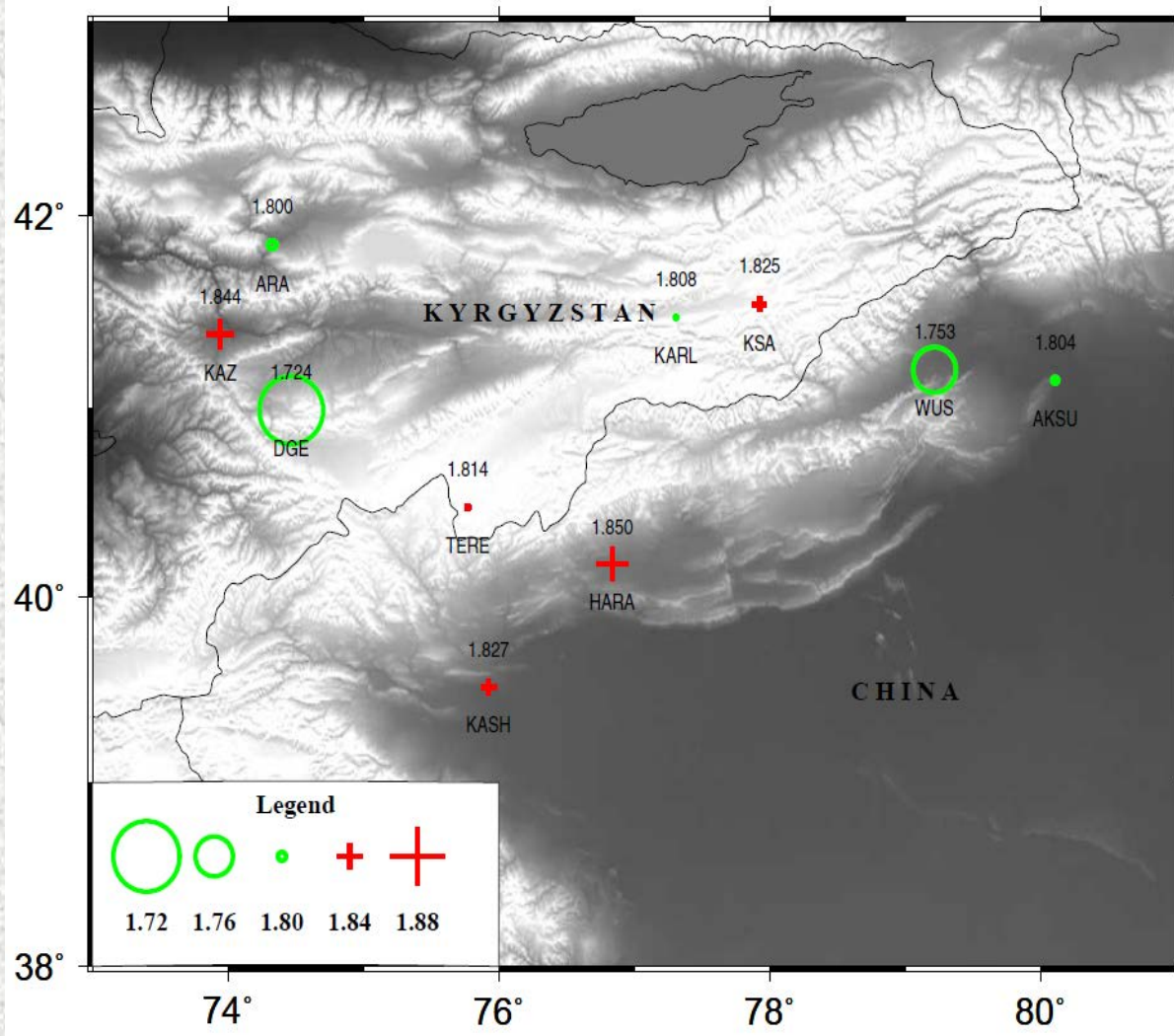
■ The resulting average crustal thickness beneath Tien Shan is about (53) km, which is consistent with previous determinations.

■ The crustal thickness varies in a range from (36) km (east of the Talas Fergana fault) to about 68 km (northwestern corner of the Tarim basin).

■ The crust thickens in the north and the southwest side of Tien Shan, while the central part has fairly a thin crust.

Figure 18: Resulting crustal thickness (H). Circles represent stations with a smaller thickness and pluses are stations with a larger thickness. Solid symbols are category (A) stations and dotted ones are the category (B) stations.

Poisson's ratio (σ) and (V_p/V_s):



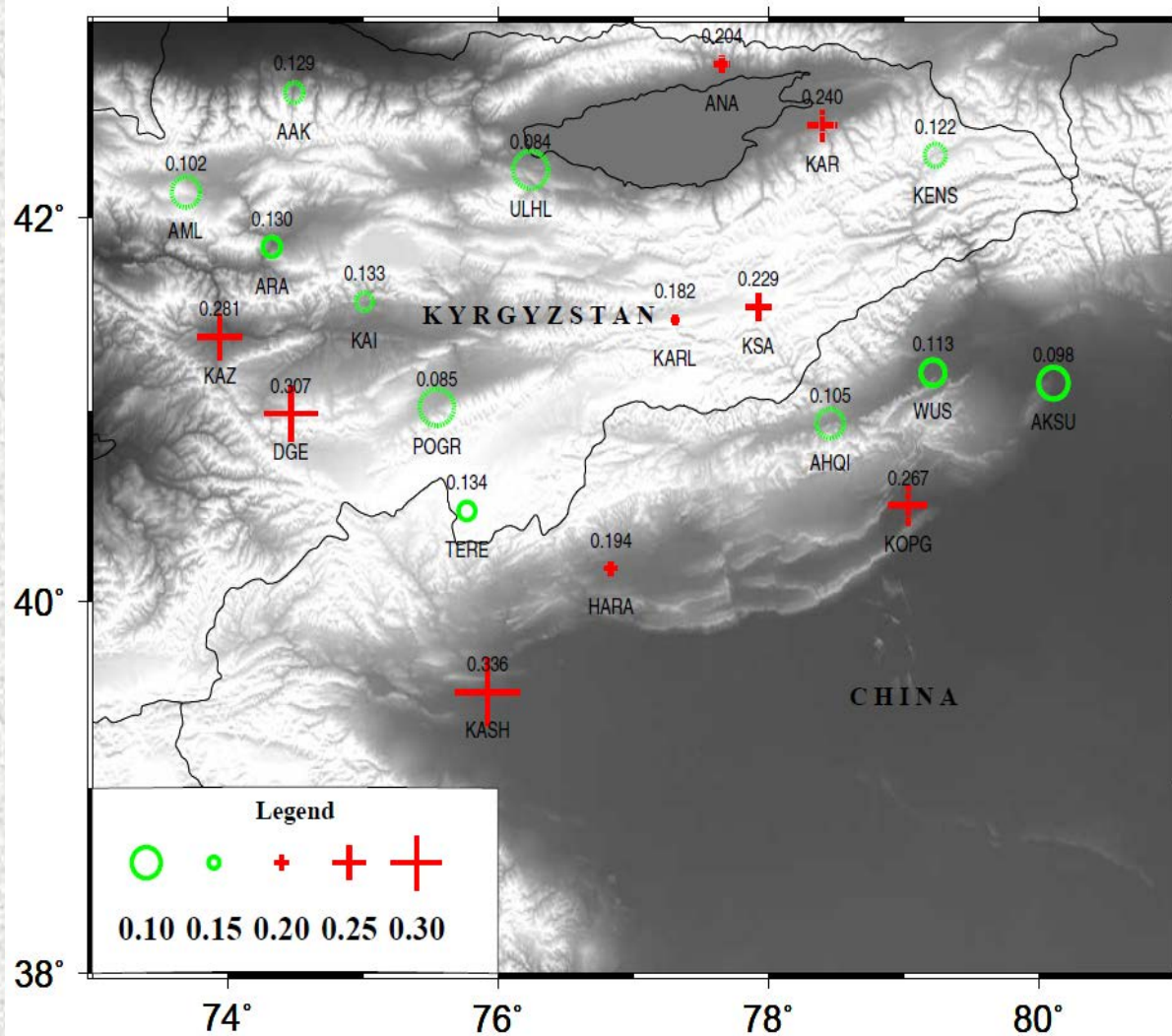
■ The resulting (V_p/V_s) values ranges from (1.72) to (1.85), with a mean of (1.81) while Poisson's ratio ranges from (0.24-0.29).

■ The northwestern corner of the Tarim basin has the highest values (1.81-1.85).

■ The regions of thicker crust show high values of (V_p/V_s).

Figure 19: Resulting crustal V_p/V_s (Φ) for category A stations.

(R) Moho sharpness:



■ The (R) values have a mean of (0.14) with a range of (0.084-0.366).

■ (R) value is the largest at the northwestern corner of the Tarim basin, and decrease gradually towards the northwest.

Figure 20: Resulting ratio (R) of the stacking amplitude corresponding to the optimal pair of (H, Φ) over that of direct P-wave on the radial component. R is calculated for all the stations.

Interpretation:

- **The largest crustal thickness (68 km) is found in the Tarim-Tien Shan junction zone due to the underthrusting of the Tarim basin towards south of Tien Shan.**
- **The observation of thin crust (36 km) area between the Talas-Fergana fault and east of Issyk Kul indicate that part of the lower crust is removed by delamination.**
- **The crustal thickness values increases from north to south, with increasing elevation.**

Interpretation contd ...

- **The high (Φ) and (H) values observed in category (A) stations are due to intrusion of basaltic material in the crust from the mantle below.**
- **Category (A) stations have high values of Poisson's ratio ranging from (0.24- 0.29) indicate intermediate rock type in the lower crust.**
- **The regions of thickened crust show high values of (V_p/V_s).**
- **The high average value of (1.81) indicate mafic crustal composition.**

Conclusions:

- ▲ The average crustal thickness for Tien Shan is (53) km.
- ▲ Tien Shan is characterized by high values of (Φ) suggesting a mafic crustal composition.
- ▲ Tien Shan has a high Poisson's ratio (0.27) indicate intermediate rock type in the lower crust.
- ▲ Central part of Tien Shan is mostly different from the southern and the northern parts in terms of crustal thickness and Moho sharpness.
- ▲ The crust thickness with increasing elevation from south to north.
- ▲ Lower values of (R) suggest the Moho is disturbed as a result of intrusion.
- ▲ The high values of (Φ) in the northwestern corner of the Tarim basin are most likely due to the intrusion of basalt into the crust.
- ▲ The collision zone between Tien Shan and Tarim Basin has the thickest crust.
- ▲ Mafic addition is assumed to be a dominant process in the modification of crustal composition.

Thank you